Applied Surface Science 571 (2022) 151311

Contents lists available at ScienceDirect

Applied Surface Science

journal homepage: www.elsevier.com/locate/apsusc

Full Length Article

Radical flux control in reactive ion beam etching (RIBE) by dual exhaust system

Doo San Kim [a,1], Yun Jong Jang [a,1], Ye Eun Kim [a], Hong Seong Gil [a], Hee Ju Kim [a], You Jin Ji [a], Hyung Yong Kim [c], In Ho Kim [c], Myoung Kwan Chae [c], Jong Chul Park [c], Geun Young Yeom [a,b,*]

[a] School of Advanced Materials Science and Engineering, Sungkyunkwan University, Suwon 16419, Republic of Korea
[b] SKKU Advanced Institute of Nano Technology (SAINT), Sungkyunkwan University, Suwon 16419, Republic of Korea
[c] Process Development Team, Semiconductor R&D Center Samsung Electrics Co., Ltd., Republic of Korea

ARTICLE INFO

Keywords:
reactive ion etching (RIE)
reactive ion beam etching (RIBE)
Radical
Ion
Exhaust
CF_4
Etch profile

ABSTRACT

Radicals generated during reactive ion etching (RIE) cannot be electrically controlled, causing isotropic etching and chemical damage to the sidewall of the etched feature during the etching process. In this study, using a reactive ion beam etcher (RIBE) installed with a dual exhaust system, where an additional exhaust valve was introduced to pump out radicals from the inductively coupled plasma (ICP) source chamber in addition to the conventional main gate valve in the process chamber, the radical flux relative to ion flux during the RIE process has been controlled and the effect of additional exhausting through the ICP source chamber for the control of radical flux relative to ion flux on the properties of etching has been investigated using CF_4 gas. The results showed that the additional exhausting of the radicals through the ICP source chamber not only decreased the ICP source chamber pressure but also decreased the ratio of radical flux to ion flux to the substrate. The lower ICP source chamber pressure could be also obtained without additional exhausting through the ICP source chamber by decreasing the CF_4 gas flow rate to the ICP source chamber, however, the lower ratio of radical flux to ion flux was observed for the dual exhaust system. It is believed that, for the next generation RIBE, multiple exhausting is beneficial for anisotropic etching of nanoscale features by controlling the radical flux to the sidewall and ion flux to the bottom of a nanoscale feature during the etching.

1. Introduction

With the increase of semiconductor device integration, the minimum line width of the semiconductor pattern has been continuously decreased and reached the level of several nanometers now. For the nanometer scale device processing, the difficult etching processes such as precise control of the etch thickness, high etch selectivity with the mask materials, vertical etch profile, low surface roughness, and low chemical etch damage are required.[1,2] To satisfy the etch requirements, various etch techniques such as pulsed plasma etching [3–5], atomic layer etching [6–10], cryogenic etching [11–13], ion beam etching [14,15], and neutral beam etching [16,17] are being investigated. These etch techniques require the understanding of the physical and chemical interactions occurring in the plasma and substrate, and also require independent and precise control of ions and radicals generated in the plasma.

In general, during the reactive ion etching (RIE) processes, the flux and the direction of the ions can be controlled electrically by adjusting the source power and bias power.[18–20] And the radical flux can be also controlled by adjusting the source power but the direction of the radicals cannot be controlled by any method. Therefore, during the etch processes, radicals react not only with the bottom surface of the etch feature but also with the sidewall of the etch feature, and, if volatile compounds are formed on the sidewall surface, less anisotropic etching will be resulted. In addition, radicals can penetrate inside the pattern and cause chemical damage to the pattern sidewall material.[21,22] These damages caused by radicals tends to show a greater effect on etching as the pattern size is decreased, so, the need for the independent control of radicals and ions in the etching process is gradually increasing.

* Corresponding author at: School of Advanced Materials Science and Engineering, Sungkyunkwan University, 2066 Seobu-ro, Jangan-gu, Suwon-si, Gyeonggi-do 16419, Republic of Korea.
E-mail addresses: entks92@naver.com (D.S. Kim), gyyeom@skku.edu (G.Y. Yeom).
[1] These authors contributed equally to this work.

https://doi.org/10.1016/j.apsusc.2021.151311
Received 25 May 2021; Received in revised form 2 September 2021; Accepted 13 September 2021
Available online 14 September 2021

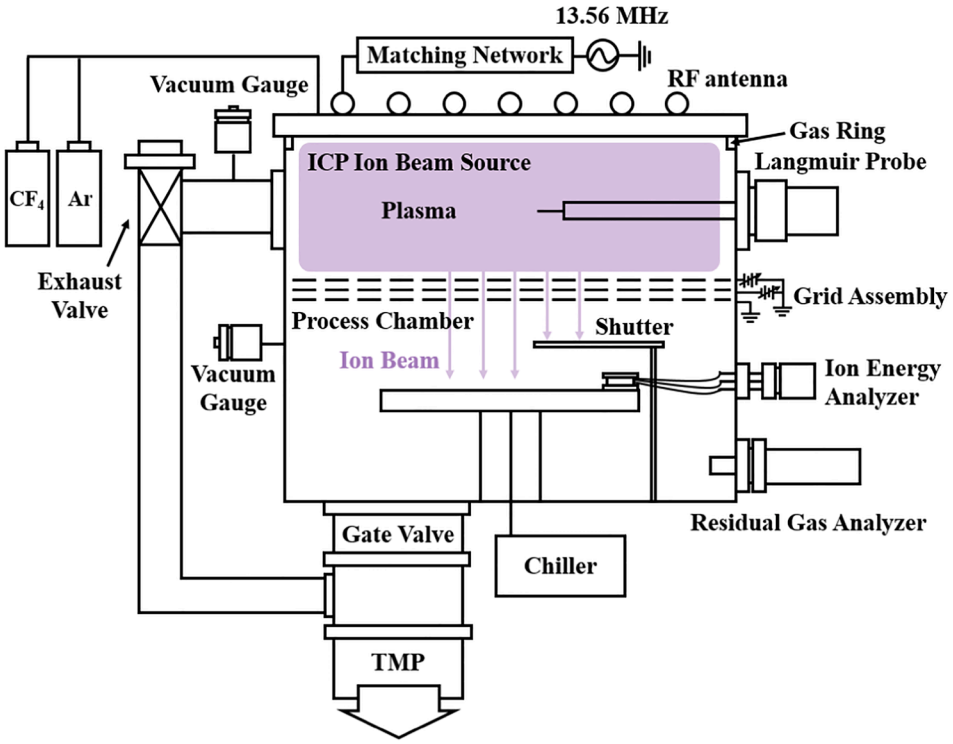

Fig. 1. Schematic diagram of the reactive ion beam etcher (RIBE) with dual exhausting for radical flux control.

In this study, a reactive ion beam etching (RIBE) system was used to study the effect of relative fluxes of ions and radicals reaching the substrate during RIE processes. In the case of the RIBE system, the plasma generation region and the substrate processing region can be separated by using a remote plasma source, and ions and radicals are extracted from the plasma source to the substrate processing chamber using a grid assembly, enabling easier control of the relative flux between ions and radicals to the substrate used in the RIE processes. To control the relative flux between ions and radicals to the substrate, a dual exhaust system was introduced in the RIBE system to control the amounts of radicals generated from the plasma, therefore, to control the fluxes of radicals and ions to the substrate during the RIE process. Using the dual exhaust system in the RIBE, the flux ratio of radicals and ions to the substrate could be varied and, by etching a nanoscale patterned silicon with a CF_4 plasma, the effect of ratio of radical flux to ion flux on the etch profile could be confirmed.

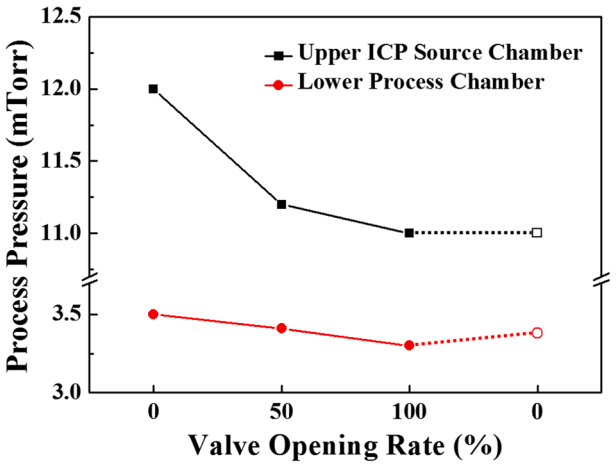

Fig. 2. Pressure in the upper ICP source chamber and lower process chambers according to the control of the exhaust valve opening in the ICP source chamber. Process CF_4 gas was fed to the ICP source chamber.

2. Experimental

A schematic diagram of the reactive ion beam etcher (RIBE) used in the experiment is shown in Fig. 1. CF_4 gas was used to study the radical control effect, and 13.56 MHz, 300 W radio frequency (RF) was applied to inductively coupled plasma (ICP) ion beam source for plasma generation. A three-grid assembly that extracts ions from the plasma and controls the energy of the ions was located under the ICP source. The grid was made of graphite with the diameter of 14 cm, the thickness of 1 mm, and the hole diameter of 2 mm. Also, the spacing between the grids was ~ 1.7 mm. The grid assembly consisted of the 1st grid (located close to the plasma) that controls the energy of ions extracted from the plasma by applying positive DC voltage, the 2nd grid (located between 1st grid and 3rd grid) that controls the flux of ions extracted by applying negative DC voltage (more negative voltage to the 2nd grid can increase the ion flux but, a high negative voltage can increase the possibility of arcing between the grids), and the 3rd grid (located near the substrate) connected to the ground. A shutter and a substrate were placed under the grid assembly, and the substrate was kept at room temperature (RT). The base pressure of the ion beam etching (IBE) chamber was approximately 2.0×10^{-5} Torr. In order to extract the reactive ion beam from the CF_4 ICP source and to control the fluxes of reactive radicals reaching the substrate at the same time, an exhaust hole with a diameter of 25 mm connected with a valve was formed in the ICP ion beam source chamber, and it was connected to the turbo molecular pump (TMP) adapter at the bottom of the chamber. Therefore, the radicals generated in the ICP ion beam source chamber could be additionally removed from the ICP chamber through the exhaust valve without removing through the main gate valve in the process chamber. In addition, by varying the exhaust hole size using the valve, the radical amount reaching the substrate by passing through the grid assembly holes could be controlled.

The pressure changes with the variation of the exhaust valve opening size were monitored with pressure gauges (MKS baratron gauge, type 627) located at the ICP source chamber and the process chamber.

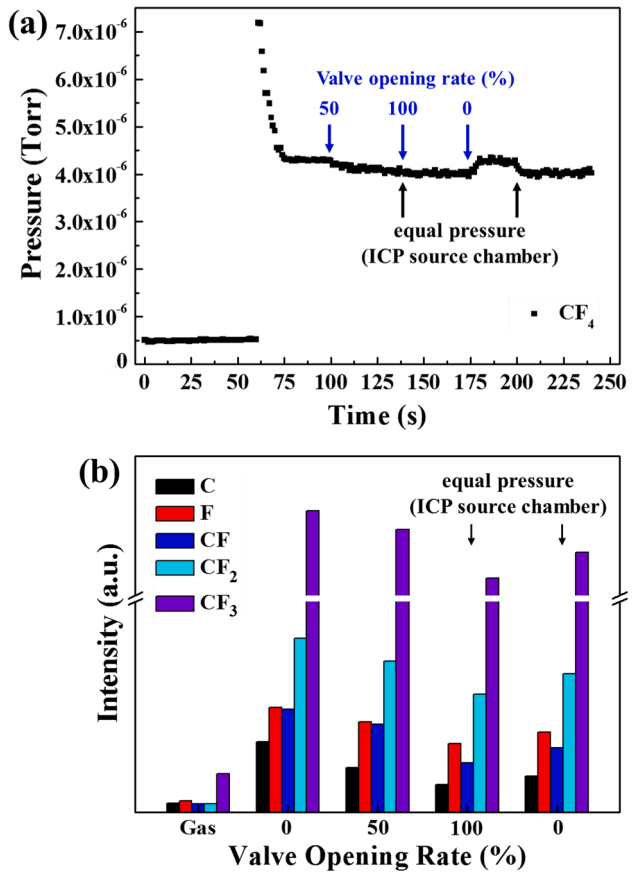

Fig. 3. (a) Pressure measured at RGA while adjusting exhaust valve. (b) Changes in the amount of C, F, and CF_x radicals generated by CF_4 plasma for different exhaust valve opening ratios and pressure (for 0 % exhaust valve opening).

Residual gas analyzer (RGA, SRS 200) was used to measure the amount of C, F, and CF_x radicals reaching the process chamber while controlling the pressure through the exhaust valve at the ICP ion beam source chamber. In addition, a single Langmuir probe (APL-150, Impedans) was installed at the ICP source chamber to measure the change in plasma characteristics generated during the control of the opening of the exhaust valve. The probe tip was made of tungsten, 0.4 mm in diameter and 24 mm in length. A retarding grid ion energy analyzer was installed on the substrate location to measure the energy and flux changes of the

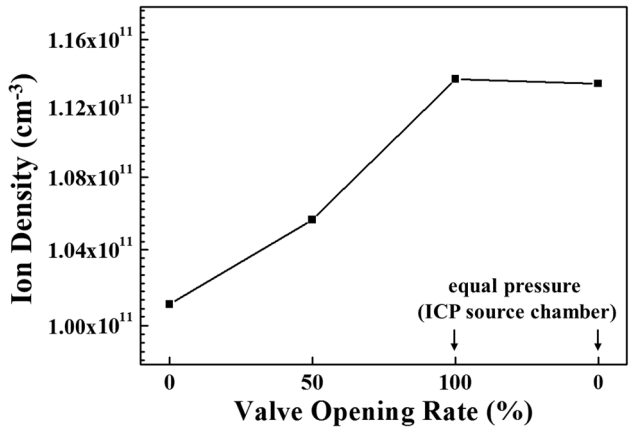

Fig. 4. Ion densities measured in the ICP source chamber using a single Langmuir probe by controlling the exhaust valve opening ratios and pressure (for 0 % exhaust valve opening).

ion beam extracted from the ICP ion beam source. The differences in the surface composition of etched silicon sidewall for the different exhaust valve opening were observed using X-ray photoelectron spectroscopy (XPS; Thermo VG, MultiLab 2000, Mg Kα source). The patterned silicon etch profiles for different exhaust valve opening were observed using a scanning electron microscope (SEM; Hitach S-8700).

3. Results and discussion

Fig. 2 shows the pressure changes of ICP ion beam source chamber and process chamber measured as a function of the additional exhaust valve opening ratio installed at the ICP ion beam source chamber in addition to the gate valve at the bottom of the process chamber. 65 sccm CF_4 gas was flowed uniformly from the ICP ion beam source chamber and the pressures were measured both at the ICP source chamber and at the process chamber while varying the exhaust valve ratio from 0 % (full close) to 100 % (full open) and the results are shown in Fig. 2. As shown in Fig. 2, when the exhaust valve was closed, the ICP source chamber pressure was 12 mTorr, and, as the exhaust valve opening ratio is increased to 50 and 100 %, the ICP source chamber pressure was decreased to 11.2 and 11 mTorr, respectively. In the case of process chamber, the pressure was lower as 3.5, 3.4, and 3.3 mTorr for 0, 50, and 100 % of exhaust valve opening due to the existence of main gate valve below the process chamber while limiting the conductance of the gas flow from the ICP source chamber by the grid assembly. In fact, the lower ICP source chamber pressure of 11 mTorr, which is the same pressure for 100 % exhaust valve opening, can be also obtained without opening the exhaust valve at the ICP source chamber and by lowering the CF_4 gas flow rate to 58 sccm and, in this case, the process chamber showed 3.4 mTorr which is a little higher than the pressure obtained with 100 % of exhaust valve opening. Therefore, while keeping the same operating pressure of the ICP ion source chamber, the process chamber pressure could be varied by controlling the exhaust valve opening ratio, and which shows the possibility in controlling the ratio of radicals and ions at the substrate on the process chamber.

Fig. 3(a) shows the pressure of CF_4 measured with the RGA installed at the sidewall of the process chamber during the CF_4 gas flow to the ICP ion beam source chamber. As shown in Fig. 3(a), when no gas was introduced to the ICP source chamber, the pressure measured at the RGA was ~ 5.0×10^{-7} Torr (0 ~ 60 s). After the CF_4 gas flow of 65 sccm to reach 12 mTorr in the ICP ion source chamber, the pressure was initially increased and reached at ~ 4.3×10^{-6} Torr without opening the exhaust valve (60 ~ 100 s). When the exhaust valve was opened 50 %, the pressure was decreased to ~ 4.1×10^{-6} Torr (100 ~ 140 s) and the further opening of the valve to 100 % decreased the pressure further to ~ 4.0×10^{-6} Torr (140 ~ 175 s). When the exhaust valve was closed, the pressure of RGA was returned to ~ 4.3×10^{-6} Torr (175 ~ 200 s). In addition, when the CF_4 pressure in the ICP ion source chamber was decreased to 11 mTorr by reducing the CF_4 flow rate at the ICP ion source chamber while the exhaust valve is closed, the pressure of the RGA was decreased to 4.0 ~ 4.1×10^{-6} Torr (200 ~ 240 s). Therefore, the pressures measured at the RGA showed the similar trends to those measured with the pressure gauges at the ICP ion beam chamber and the process chamber. Using the RGA, the radical species dissociated from the CF_4 plasmas were also compared for the different exhaust valve opening ratios. To generate the CF_4 plasma in the ICP ion beam source, 300 W of 13.56 MHz was applied to the ICP source. Because, RGA makes fragmentation of molecules during the measurement of species, the species measured just by flowing CF_4 gas without generating CF_4 plasma were also compared as a reference. In the case of the CF_4 gas flow without generating plasma, a small mass peak related to CF_3 was observed while no noticeable peaks related to C, F, CF, and CF_2 could be observed. However, as shown in Fig. 3(b), when the plasma was turned-on, the dissociated species such as CF_3, CF_2, CF, F, and C were observed with RGA (the most abundant species was CF_3) and, as the exhaust valve opening ratio was increased from 0 to 100 %, the intensities of the

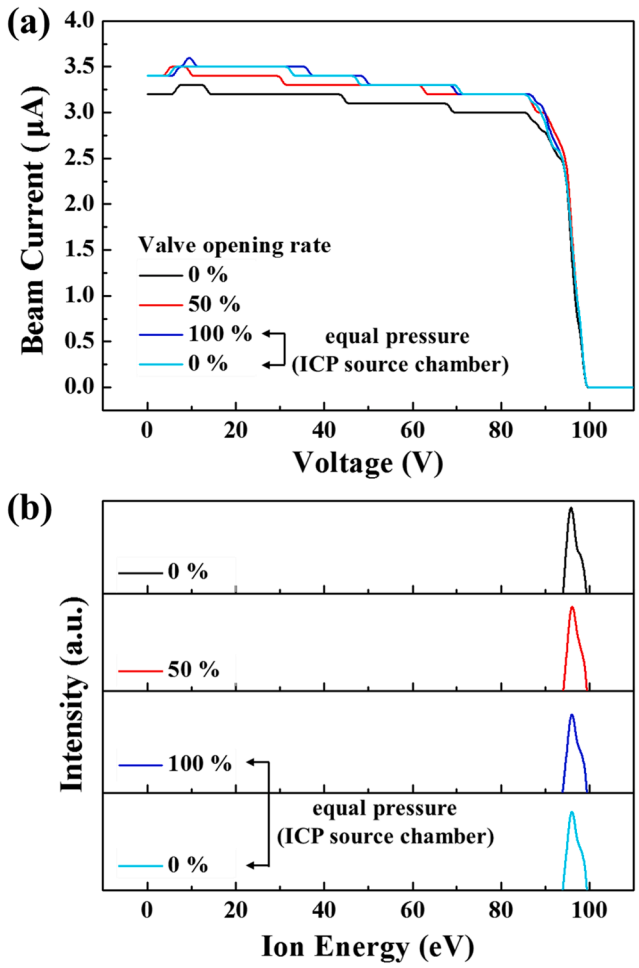

Fig. 5. (a) Ion beam currents and (b) Ion energy distributions to the substrate according to exhaust valve opening ratios and pressure (for 0 % exhaust valve opening) measured by a retarding grid ion energy analyzer.

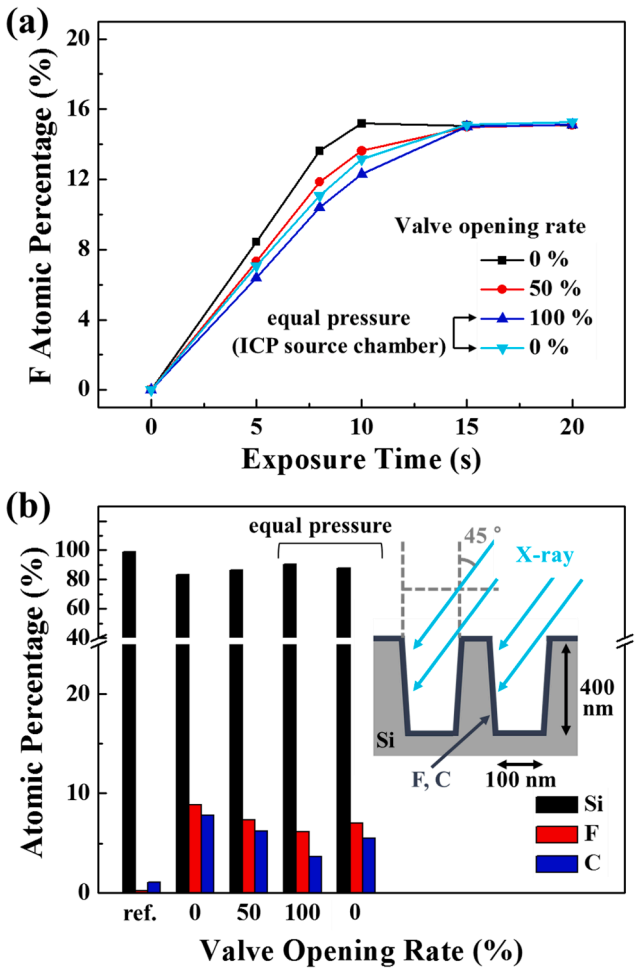

Fig. 6. (a) F atomic percentage adsorbed on flat silicon surface as a function of radical exposure time and (b) adsorption amount of F and C radicals on the sidewall of the silicon pattern measured by XPS for different exhaust valve opening ratios and pressure (for 0 % exhaust valve opening).

dissociated species were also decreased indicating the decreased radicals in the process chamber with the increased exhaust valve opening ratio. When the CF_4 pressure at the ICP ion beam source chamber was decreased to 11 mTorr by decreasing the CF_4 flow rate to 58 sccm without opening the exhaust valve (the same pressure with the exhaust value opening ratio of 100 % while flowing 65 sccm CF_4), the intensities of dissociated species were also decreased but those intensities were higher than those observed with exhaust valve full open while flowing 65 sccm CF_4. It indicates that lower radicals can be obtained in the process chamber while keeping the same pressure at the ICP ion beam source by using the exhaust valve at the ICP ion source chamber rather than reducing gas flow rate to the ICP ion source chamber.

The ion densities in the ICP ion source chamber were measured using a Langmuir probe installed at the ICP ion beam source chamber for different exhaust opening ratios and the results are shown in Fig. 4. The CF_4 plasma conditions in Fig. 3 were used and, for the ion density measurement, the ion mass of CF_3^+ was used for the Langmuir probe measurement because CF_3^+ is the major ion species in the CF_4 plasma. As shown in Fig. 4, the ion density was increased with the increase of exhaust valve opening ratio by showing 1.01×10^{11}, 1.05×10^{11}, and 1.14×10^{11} cm^{-3} for 0, 50, and 100 % of exhaust valve opening, respectively. When the ion density of the CF_4 plasma was measured at 11 mTorr by reducing the CF_4 flow rate while closing the exhaust valve, the ion density of $\sim 1.13 \times 10^{11}$ cm^{-3} which is similar to that observed at 11 mTorr obtained by opening 100 % of the exhaust valve could be measured. Therefore, the ion density in the ICP ion beam source chamber was more related to the pressure in the chamber and was not changed with exhausting gas through the ICP ion beam source chamber.

While generating the CF_4 plasmas in the ICP ion beam source with the conditions of Fig. 3(b), the flux and energy distribution of the ions extracted from the ICP ion beam source were measured using a retarding grid ion energy analyzer at the substrate location in the process chamber by applying voltages to the grid assembly and the results are shown in Fig. 5(a) for ion flux measured as a function of ion energy and (b) for ion energy distribution. For the measurement, +80 V was applied to the 1st grid located near the ICP source and −200 V was applied to the 2nd grid while the 3rd grid was grounded. As shown in Fig. 5(a), when the exhaust valve was closed at 12 mTorr, the beam current (that is, ion flux to the substrate) was the lowest at ~ 3.2 μA and, with the increase of the exhaust valve opening ratio to 100 %, the beam current to the substrate was increased and, the beam current measured with the exhaust valve closed with the CF_4 flow rate of 58 sccm was similar to the that with 100 % of the exhaust valve ratio for the CF_4 flow rate of 65 sccm. The measured beam currents were similar to the ion densities in the ICP ion beam source for different exhaust valve opening ratios shown in Fig. 4. The ion energy distribution incident to the substrate can be obtained by differentiating the beam current in Fig. 5(a) with the voltage and the results are shown in Fig. 5(b). As shown in Fig. 5(b), the energy distributions of the ions extracted from the ICP ion beam source by the grid assembly and arrived at the substrate were in the range of 92 ~ 100 eV which is a little higher than 1st grid voltage due to the plasma potential

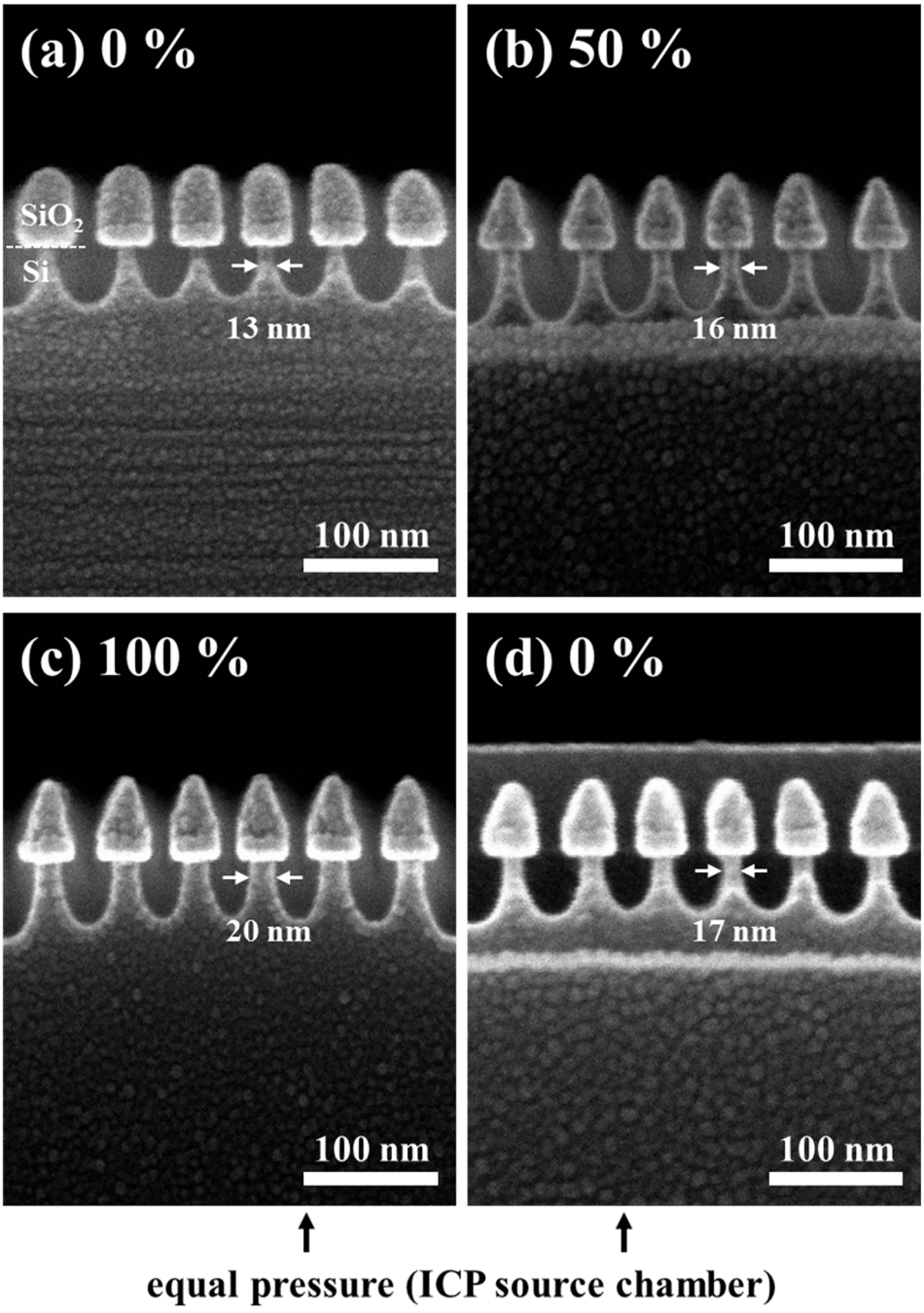

Fig. 7. SEM images of silicon pattern etched using RIBE. (a), (b), and (c) for 0, 50, and 100 % of exhaust valve opening ratios at 65 sccm gas flow rate, respectively, and (d) for 0 % of exhaust valve opening ratio with the same operating pressure as (c) by reducing gas flow rate. Silicon was patterned with 40 nm width SiO_2 (40 nm)/ SiN (20 nm) and was etched with CF_4/Ar = 1:4, 12 mTorr, RF 300 W, and for 12 min while applying voltages to the grid system (1st grid V = +80 V, 2nd grid V = -200 V).

in the plasmas. Therefore, the ion energy distributions were similar for all of the cases regardless of exhaust valve ratios and pressures.

In addition to ion flux and energy to the substrate, the radical flux arriving at the substrate was measured by XPS in Fig. 6(a) and (b) by estimating the adsorption characteristics of the F radical on silicon substrate and by measuring the atomic percentages of the radicals adsorbed on the sidewall of the patterned silicon, respectively, for the conditions in Fig. 3(b). For the XPS analysis, the samples were exposed to air as it moved from the process chamber to the analysis chamber, therefore, there was a possible change in the surface condition during the air exposure. However, in order to minimize the change in the surface condition during the transport, the samples were always prepared immediately before the analysis and the exposure time to air was about a few minutes. To observe the radicals arriving at the substrate only, the ions extracted from the ICP ion beam source were blocked by a shutter installed below the ICP ion beam source in addition to applying no voltages to the grid assembly. As shown in Fig. 6(a), when the fluorine adsorbed on silicon surface was measured using XPS for different exhaust valve opening ratios, adsorbed fluorine was saturated on the silicon surface after the exposure to the silicon surface for more than 15 s, however, the rate of atomic F adsorption was lower with increasing the exhaust valve opening ratios by showing 15.2, 13.6, and 12.3 % fluorine percentage on silicon surface after 10 s exposure for 0, 50, and 100 % of exhaust valve opening. In the case of the condition with the reduced CF_4 gas flow rate with 0 % exhaust valve opening to have the same pressure with the case with 100 % exhaust valve opening, the adsorbed F was also saturated after 15 s but the rate of atomic F adsorption was faster compared to the case with 100 % exhaust valve opening by showing 13.2 % of fluorine percentage on silicon surface after 10 s of exposure time. To estimate the radicals adsorbed on the

sidewall of the patterns, in Fig. 6(b), a patterned silicon with 400 nm deep trenches was exposed to the radicals for 10 s as in Fig. 6(a) and the composition of the silicon trench surface was measured using XPS with a tilted angle of 45° for different exhaust valve opening ratios. As shown in Fig. 6(b), by the exposure to CF_4 plasma, carbon and fluorine were detected on the silicon trench surface in addition to silicon by XPS and the higher exhaust valve opening ratios showed lower carbon and fluorine percentages on the sidewall of the silicon trenches. For the same ICP ion beam source chamber pressure conditions with 0 and 100 % exhaust valve opening, the condition with 100 % exhaust valve opening showed lower adsorption of radicals on the sidewall of the silicon trenches compared to the condition with 0 % exhaust valve opening. Therefore, from Fig. 6(a) and (b), it is found that, the radical flux to the sidewall of the patterned feature could be varied by controlling gas flow additionally at the ICP ion beam source chamber using an exhaust valve while maintaining the ion flux and energy to the substrate.

To study the effect of the radical flux compared to the ion flux to the processing chamber on the nanoscale etching, silicon patterned with 40 nm width SiN (20 nm)/SiO_2 (40 nm) hardmask was etched using the ICP ion beam source (CF_4/Ar = 1:4, 12 mTorr, RF 300 W, 12 min with the grid voltages of 1st grid + 80 V, 2nd grid −100 V, and 3rd grid ground), and the results are shown in Fig. 7(a)~(c) for 0, 50, and 100 % of exhaust valve opening ratios at 65 sccm gas flow rate, respectively, and (d) for 0 % of exhaust valve opening with the same operating pressure as (c) by reducing gas flow rate. As shown in Fig. 7(a)~(c), with the increase of exhaust valve opening ratios, the patten width near the center of the silicon etched features were decreased from 13, 16, and 20 nm, respectively, and the etch profiles were improved more anisotropically through lowering the operating pressure of the ICP source chamber. In these cases, the change of ICP source chamber pressure not only changes the radical flux but also changes the ion flux to the substrate as shown in Fig. 5. However, when the silicon etch profile of the condition (c) was compared with that of the condition (d), even though the same operating pressure was maintained at the ICP source chamber, the radical flux is higher for (d) compared to (c) while the ion fluxes/energies are similar as shown in Fig. 5, and better silicon etch profile could be observed for (c). (During the etching process, with increasing the valve opening ratio from 0 % of Fig. 7(a) to 100 % of Fig. 7(c), more etching of SiN/SiO_2 mask edge was observed due to the increase of ion flux to the substrate. However, the etch amounts of the SiN/SiO_2 mask edges for Fig. 7(c) and (d) were similar due to the similar ion fluxes/energies.) Therefore, it is believed that, in the nanoscale anisotropic etching, the control of radical flux compared to ion flux is important and, for RIBE, by removing the radicals generated in the ICP ion beam source chamber by introducing dual exhaust system in addition to decreasing the operating pressure, more anisotropic etch profiles could be obtained by increasing the ratio of ion flux over radical flux to the substrate.

4. Conclusions

In the dry etch process, precise control of ions and radicals is required to perform nano-scale etching. In this study, a dual exhaust system was introduced to control radicals for RIBE, and the effects of ion flux and radical flux to the substrate on nanoscale anisotropic etching were investigated using CF_4. An exhaust valve was installed in the ICP ion source chamber of the RIBE system and, by increasing the exhaust valve opening ratio, radicals generated in the ICP source chamber could be decreased before it was transferred to the processing chamber while the ions generated in the ICP source chamber could be transferred to substrate in the processing chamber without changing the energy and flux of the ions through the grid system of the ICP ion beam source. In fact, the decrease of radicals in the ICP source chamber, and therefore, lower radicals in the processing chamber, can be also obtained with decreasing the operating pressure in the ICP source chamber. However, when the 100 % exhaust valve opening was compared with the 0 % exhaust valve opening (that is, no additional exhaust valve in the ICP source chamber with a reduced gas flow rate for the same operating pressure), the ratio of radical flux to ion flux was higher for the case with the 100 % exhaust valve opening in the ICP source chamber. The significant decrease of radical flux compared to ion flux is more required for the next generation nanoscale etching for vertical etching. And, it is believed that the removal of radicals by introducing the additional exhaust valve in the ICP source chamber for the RIBE system can be useful for the next generation nanoscale anisotropic etching in addition to the decrease of operating pressure.

CRediT authorship contribution statement

Doo San Kim: Conceptualization, Methodology, Validation, Writing – original draft. **Yun Jong Jang:** Investigation. **Ye Eun Kim:** Investigation. **Hong Seong Gil:** Investigation. **Hee Ju Kim:** Resources. **You Jin Ji:** Resources. **Hyung Yong Kim:** Funding acquisition. **In Ho Kim:** Funding acquisition. **Myoung Kwan Chae:** Funding acquisition. **Jong Chul Park:** Funding acquisition. **Geun Young Yeom:** Supervision, Writing – review & editing.

Declaration of Competing Interest

The authors declare that they have no known competing financial interests or personal relationships that could have appeared to influence the work reported in this paper.

Acknowledgements

This work was supported by the National Research Foundation of Korea (NRF) grant funded by the Korea government (MSIT) (2018R1A2A3074950) and the Samsung Electronics' university R&D program [Development of small pitch MTJ patterning process using RIBE] and Samsung Electronics Co., Ltd. (IO201211-08086-01).

References

[1] H. Lee, Review of inductively coupled plasmas: Nano-applications and bistable hysteresis physics, Appl. Phys. Rev. 5 (2018), 011108.
[2] K. Eriguchi, Modeling of defect generation during plasma etching and its impact on electronic device performance—plasma-induced damage, J. Phys. D: Appl. Phys. 50 (2017), 333001.
[3] D.J. Economou, Pulsed plasma etching for semiconductor manufacturing, J. Phys. D: Appl. Phys. 47 (2014), 303001.
[4] M. Haass, M. Darnon, G. Cunge, O. Joubert, D. Gahan, Silicon etching in a pulsed HBr/O_2 plasma. I. Ion flux and energy analysis, J. Vac. Sci. Technol. B 33 (2015), 032202.
[5] S.G. Kim, K.C. Yang, Y.J. Shin, K.N. Kim, D.W. Kim, J.Y. Lee, Y.H. Kim, G.Y. Yeom, Etch characteristics of Si and TiO_2 nanostructures using pulse biased inductively coupled plasmas, Nanotechnol. 31 (2020), 265302.
[6] G.S. Oehrlein, D. Metzler, C. Li, Atomic Layer Etching at the Tipping Point: An Overview, ECS J. Solid State Sci. Technol. 4 (6) (2015) N5041–N5053.
[7] S. Tan, W. Yang, K.J. Kanarik, T. Lill, V. Vahedi, J. Marks, R.A. Gottscho, Highly Selective Directional Atomic Layer Etching of Silicon, ECS J. Solid State Sci. Technol. 4 (6) (2015) N5010–N5012.
[8] D.S. Kim, J.E. Kim, W.O. Lee, J.W. Park, Y.J. Gill, B.H. Jeong, G.Y. Yeom, Anisotropic atomic layer etching of W using fluorine radicals/oxygen ion beam, Plasma Process Polym. 16 (2019) 1900081.
[9] A. Ranjan, M. Wang, S.D. Sherpa, V. Rastogi, A. Koshiishi, P.L.G. Ventzek, Implementation of atomic layer etching of silicon: Scaling parameters, feasibility, and profile control, J. Vac. Sci. Technol. A 34 (2016), 031304.
[10] K.J. Kanarik, S. Tan, W. Yang, T. Kim, T. Lill, A. Kabansky, E.A. Hudson, T. Ohba, K. Nojiri, J. Yu, R. Wise, I.L. Berry, Y. Pan, J. Marks, R.A. Gottscho, Predicting synergy in atomic layer etching, J. Vac. Sci. Technol. A 35 (2017) 05C302.
[11] R. Dussart, T. Tillocher, P. Lefaucheux, M. Boufnichel, Plasma cryogenic etching of silicon: from the early days to today's advanced technologies, J. Phys. D: Appl. Phys. 47 (2014), 123001.
[12] M.W. Pruessner, W.S. Rabinovich, T.H. Stievater, D. Park, J.W. Baldwin, Cryogenic etch process development for profile control of high aspect-ratio submicron silicon trenches, J. Vac. Sci. Technol. B 25 (2007) 21.
[13] S. Tinck, T. Tillocher, R. Dussart, A. Bogaerts, Cryogenic etching of silicon with SF_6 inductively coupled plasmas: a combined modelling and experimental study, J. Phys. D: Appl. Phys. 48 (2015), 155204.
[14] J.E. Kim, D.S. Kim, Y.J. Gill, Y.J. Jang, Y.E. Kim, H. Cho, B. Won, O. Kwon, K. Yoon, J. Choi, J. Park, G.Y. Yeom, Etch characteristics of magnetic tunnel

junction materials using H_2/NH_3 reactive ion beam, Nanotechnol. 32 (2021), 055301.
[15] N. Gosset, M. Boufnichel, E. Bahette, W. Khalfaoui, R. Ljazouli, V.G. Perrigouas, R. Dussart, Single and multilayered materials processing by argon ion beam etching: study of ion angle incidence and defect formation, J. Micromech. Microeng. 25 (2015), 095011.
[16] S. Samukawa, A Neutral Beam Process for Controlling Surface Defect Generation and Chemical Reactions at the Atomic Layer, ECS J. Solid State Sci. Technol. 4 (6) (2015) N5089–N5094.
[17] D.H. Yun, J.W. Park, H.S. Kim, J.H. Mun, S.O. Kim, K.N. Kim, G.Y. Yeom, Improvement of a block co-polymer (PS-b-PMMA)-masked silicon etch profile using a neutral beam, Nanotechnol. 27 (2016), 384002.
[18] R.J. Hoekstra, M.J. Kushner, Predictions of ion energy distributions and radical fluxes in radio frequency biased inductively coupled plasma etching reactors, J. Appl. Phys. 79 (1996) 2275.
[19] S. Imai, Bias power dependence of reactive ion etching lag in contact hole etching using inductively coupled fluorocarbon plasma, J. Vac. Sci. Technol. B 26 (2008) 2008.
[20] F. Laermer, A. Urban, C hallenges, developments and applications of silicon deep reactive ion etching, Microelectron. Eng. 67 (2003) 349.
[21] K. Ishikawa, K. Karahashi, T. Ishijima, S.I. Cho, S. Elliott, D. Hausmann, D. Mocuta, A. Wilson, K. Kinoshita, Progress in nanoscale dry processes for fabrication of high-aspect-ratio features: How can we control critical dimension uniformity at the bottom? Jpn. J. Appl. Phys. 57 (2018) 06JA01.
[22] F. Karouta, A practical approach to reactive ion etching, J. Phys. D: Appl. Phys. 47 (2014), 233501.